Manganese(II) complexes with the non-steroidal anti-inflammatory drugs naproxen and mefenamic acid. Synthesis, structure, antioxidant capacity, interaction with albumins and DNA

Filitsa Dimiza,[a] Catherine P. Raptopoulou,[b] Vassilis Psycharis,[b] Athanasios N. Papadopoulos,[c] George Psomas,[a,*]

[a] *Department of General and Inorganic Chemistry, Faculty of Chemistry, Aristotle University of Thessaloniki, P.O. Box 135, GR-54124 Thessaloniki, GREECE.*

[b] *Institute of Nanoscience and Nanotechnology, NCSR "Demokritos", GR-15310 Aghia Paraskevi Attikis, GREECE.*

[c] *Department of Nutrition and Dietetics, Faculty of Food Technology and Nutrition, Alexandrion Technological Educational Institution, Sindos, Thessaloniki, GREECE.*

Supplementary Information

S1. Single-crystal X-ray crystallography for complexes 4 and 5

A crystal of **4** with approximate dimensions 0.1 × 0.3 × 0.4 mm was mounted in air and covered with epoxy glue. Diffraction measurements were made on a Crystal Logic Dual Goniometer diffractometer using graphite monochromated Mo radiation. Unit cell dimensions were determined and refined by using the angular settings of 20 automatically centered reflections in the range $11<2\theta<21^{o}$. Intensity data were recorded using a θ-2θ scan. Three standard reflections monitored every 97 reflections showed less than 3% variation and no decay. Lorentz, polarization (and psi-scan absorption) corrections were applied using Crystal Logic software. Important crystallographic and refinement data for compounds **4** and **5** are listed in Table S1.

S2. Interaction with serum albumins

The extent of the inner-filter effect can be roughly estimated with the following formula:

$$I_{corr} = I_{meas} \times 10^{\frac{\varepsilon(\lambda_{exc})cd}{2}} \times 10^{\frac{\varepsilon(\lambda_{em})cd}{2}} \qquad \text{(eq. S1)}$$

* Corresponding author: Tel.:+30+2310997790; Fax:+30+2310997738; E-mail: gepsomas@chem.auth.gr

where I_{corr} = corrected intensity, I_{meas} = the measured intensity, c = the concentration of the quencher, d = the cuvette (1 cm), $\varepsilon(\lambda_{exc})$ and $\varepsilon(\lambda_{em})$ = the ε of the quencher at the excitation and the emission wavelength, respectively, as calculated from the UV-vis spectra of the complexes.[1]

The Stern-Volmer and Scatchard graphs are used in order to study the interaction of a quencher with serum albumins. According to Stern-Volmer quenching equation:[2]

$$\frac{Io}{I} = 1 + k_q\tau_0[Q] = 1 + K_{SV}[Q] \qquad \text{(eq. S2)},$$

where Io = the initial tryptophan fluorescence intensity of SA, I = the tryptophan fluorescence intensity of SA after the addition of the quencher, k_q = the quenching rate constants of SA, K_{SV} = the dynamic quenching constant, τ_o = the average lifetime of SA without the quencher, [Q] = the concentration of the quencher, the Stern-Volmer constant (K_{SV}, M^{-1}) can be obtained by the slope of the diagram Io/I vs [Q]. Taking $\tau_o = 10^{-8}$ s as fluorescence lifetime of tryptophan in SA, the quenching constant (k_q, $M^{-1}s^{-1}$) is calculated from the equation:

$$K_{SV} = k_q\tau_o \qquad \text{(eq. S3)}$$

From the Scatchard equation:[2]

$$\frac{\Delta I/Io}{[Q]} = nK - K\frac{\Delta I}{Io} \qquad \text{(eq. S4)}$$

where n is the number of binding sites per albumin and K is the SA-binding constant, K (in M^{-1}) is calculated from the slope in plots (ΔI/Io)/[Q] versus (ΔI/Io) and n is given by the ratio of y intercept to the slope.[2]

S3. Interaction with CT DNA

The DNA-binding constant, K_b, can be obtained by monitoring the changes in the absorbance at the corresponding λ_{max} with increasing concentrations of CT DNA and it is given by the ratio of slope to the y intercept in plots [DNA]/(ε_A-ε_f) *versus* [DNA], according to the Wolfe-Shimer equation:[3]

$$\frac{[DNA]}{(\varepsilon_A - \varepsilon_f)} = \frac{[DNA]}{(\varepsilon_b - \varepsilon_f)} + \frac{1}{K_b(\varepsilon_b - \varepsilon_f)} \qquad \text{(eq. S5)}$$

where [DNA] is the concentration of DNA in base pairs, $\varepsilon_A = A_{obsd}/[compound]$, ε_f = the extinction coefficient for the free compound and ε_b = the extinction coefficient for the compound in the fully bound form.

Cyclic voltammetry can be also used in order to calculate the corresponding equilibrium constant for the redox process. The oxidized and reduced forms are associated with a third species (DNA) in the solution using the following equation:[4]

$$\Delta E^o = E^o_{(b)} - E^o_{(f)} = 0.059 \times \log \frac{K_r}{K_{ox}} \qquad \text{(eq. S6)}$$

where $E^o_{(b)}$ and $E^o_{(f)}$ are the formal potentials of M(II)/M(I) couple in the fully bound and free complexes, respectively. K_{ox} and K_r are the binding constants for the binding of the oxidized and reduced species to DNA, respectively.

S4. Competitive studies with EB

The Stern-Volmer constant K_{SV} is used to evaluate the quenching efficiency for each compound according to the Stern-Volmer equation (eq. S2),[2] where Io and I are the emission intensities in the absence and the presence of the quencher, respectively, [Q] is the concentration of the quencher (i.e. complexes **1–5**); K_{SV} is obtained from the Stern-Volmer plots by the slope of the diagram Io/I *versus* [Q]. Taking τ_o = 23 ns as the fluorescence lifetime of the EB-DNA system,[5] the quenching constants (k_q, in $M^{-1}s^{-1}$) of the compounds can be determined according to eq. S3.

References

1 L. Stella, A.L. Capodilupo and M. Bietti, *Chem. Commun.*, 2008, 4744-4746.

2 J.R. Lakowicz, *Principles of Fluorescence Spectroscopy*, third ed., Plenum Press, New York, 2006.

3 A. Wolfe, G. Shimer and T. Meehan, *Biochemistry*, 1987, **26**, 6392-6396.

4 M.T. Carter, M. Rodriguez and A.J. Bard, *J. Am. Chem. Soc*., 1989, **111**, 8901-8911.

5 D.P. Heller and C.L. Greenstock, *Biophys. Chem*., 1994, **50**, 305-312.

Table S1. Crystallographic data for complexes **4** and **5**.

	(**4**)	(**5**)
Formula	$C_{42}H_{38}MnN_4O_5$	$C_{84}H_{88}Mn_2N_8O_{12}$
Fw	733.70	1511.50
T (K)	293(2)	160(2)
Crystal system	Triclinic	Orthorhombic
Space group	P -1	I c 2 a
a (Å)	9.539(12)	7.4374(1)
b (Å)	12.232(17)	17.2488(3)
c (Å)	15.85(2)	29.1863(5)
α (^{o})	96.85(5)	90.00
β (^{o})	96.37(5)	90.00
γ (^{o})	98.01(6)	90.00
Volume (Å^3)	1803(4)	3744.2(1)
Z	2	2
D(calc), Mg m^{-3}	1.351	1.341
Abs. coef., μ, mm^{-1}	0.418	3.303
GOF on F^2	1.028	1.147
$2\theta_{max}$(^{o})	44.0	130.0
Total / unique reflections	4740/4411	22292/2871
Rint	0.021	0.033
Reflections [I>2σ(I)]	2997	2371
parameters	478	287
$(\Delta/\sigma)_{max}$	0.003	0.001
$(\Delta\rho)_{max}/(\Delta\rho)_{min}$(e/Å^3)	0.341/-0.505	0.265/-0.402
R1/wR2 (total)	0.0969 / 0.1676	0.0564 / 0.1161
R1/wR2 [I>2σ(I)]	0.0564 / 0.1437	0.0422 / 0.0984

[a] $R_1 = \Sigma(||F_o|-|F_c||)/\Sigma(|F_o|)$ and $wR_2 = \{\Sigma[w(Fo^2-Fc^2)^2]/\Sigma[w(F_o^2)^2]\}^{1/2}$, $w=1/[\sigma^2(F_o^2)+(\alpha P)^2+bP]$ and $P = (\max F_o^2,0)+2F_c^2)/3$.

a = 0.0803, b = 1.2606 for **4**; a = 0.0464, b = 3.3599 for **5**.

[b] Flack parameter 0.024(4) for **5**.

Table S2. Selected bond distances and angles for complex **4**.

Bond	**Distance (Å)**	**Bond**	**Distance (Å)**
Mn-O(1)	2.221(4)	Mn-O(1W)	2.150(5)
Mn-O(2)	2.263(4)	Mn-N(3)	2.266(5)
Mn-O(3)	2.104(4)	Mn-N(4)	2.262(5)
O(1)-C(1)	1.271(6)	O(3)-C(21)	1.266(6)
O(2)-C(1)	1.274(6)	O(4)-C(21)	1.247(6)
Bonds	**Angle (°)**	**Bonds**	**Angle (°)**
O(1)-Mn-O(2)	58.6(1)	O(2)-Mn-O(3)	96.8(2)
O(1)-Mn-O(3)	102.6(2)	O(2)-Mn-O(1W)	156.7(1)
O(1)-Mn-O(1W)	98.1(2)	O(2)-Mn-N(3)	97.5(2)
O(1)-Mn-N(3)	153.3(2)	O(2)-Mn-N(4)	91.4(2)
O(1)-Mn-N(4)	94.2(2)	O(1W)-Mn-N(3)	104.9(2)
O(3)-Mn-O(1W)	89.4(2)	O(1W)-Mn-N(4)	88.8(2)
O(3)-Mn-N(3)	91.2(2)	N(3)-Mn-N(4)	73.2(2)
O(3)-Mn-N(4)	163.2(2)		

Table S3. Selected bond distances and angles for complex **5.**

Bond	**Distance (Å)**	**Bond**	**Distance (Å)**
Mn(1)-O(1)	2.138(3)	O(1)-C(1)	1.269(6)
Mn(1)-O(3)	2.141(7)	O(2)-C(1)	1.252(7)
Mn(1)-N(2)	2.237(6)	O(3)-C(31)	1.35(1)
Bonds	**Angle (°)**	**Bonds**	**Angle (°)**
O(1)-Mn(1)-O(1)'	177.2(3)	O(3)-Mn(1)-O(3)'	95.3(6)
O(1)-Mn(1)-O(3)	92.2(2)	O(3)-Mn(1)-N(2)	167.6(3)
O(1)-Mn(1)-O(3)'	85.9(2)	O(3)-Mn(1)-N(2)'	96.0(3)
O(1)-Mn(1)-N(2)	93.7(2)	N(2)-Mn(1)-N(2)'	73.3(3)
O(1)-Mn(1)-N(2)'	88.6(2)		

(') $-x+2, y, -z+1$.

Table S4. Antioxidant activity (% DPPH scavenging ability (RA%) in 60 min, % superoxide radical scavenging activity (ABTS%) and competition % with DMSO for hydroxyl radical ($^{\bullet}$OH%)) of the reported metal-naproxen complexes (metal = Mn(II), Cu(II), Co(II), Ni(II)).

Compound	**RA% 20 min / 60 min**	**ABTS%**	**$^{\bullet}$OH %**	**Ref.**
Hnap (naproxen)	8.03±0.32 / 8.43±0.20	87.51±0.17	89.55±0.44	1
$[Mn(nap)_2(py)_2(H_2O)_2]$, **1**	13.58±076 / 16.76±0.34	94.78±0.36	98.31±0.67	2
$[Mn(nap)_2(phen)(H_2O)]$, **2**	14.67±0.37 / 16.06±0.62	96.67±0.68	97.42±0.83	2
$[Co(nap)_2(MeOH)_4]$	not determined / 20.37±0.23	82.46±0.35	96.75±0.30	1
$[Co(nap)_2(py)_2(H_2O)_2]$	not determined / 18.90±0.22	90.22±0.28	84.98±0.35	1
$[Co(nap)_2(phen)(H_2O)_2]$	not determined / 42.42±0.13	87.32±0.17	92.46±0.22	1
$[Co(nap)_2(bipy)(H_2O)_2]$	not determined / 26.98±0.41	84.54±0.29	90.21±0.19	1
$[Cu_2(nap)_4(H_2O)_2]$	not determined / 20.16±0.23	77.74±0.39	72.84±0.05	1
$[Cu(nap)_2(py)_2(H_2O)]$	not determined / 18.66±0.29	92.12±0.13	93.40±0.22	1
$[Cu(nap)_2(phen)]$	not determined / 18.76±0.13	82.39±0.25	93.26±0.36	1
$[Cu(nap)_2(bipy)]$	not determined / 19.48±0.12	76.44±0.20	80.11±0.17	1
$[Ni(nap)_2(MeOH)_4]$	16.47±0.48 / 16.53±0.41	96.03±0.43	96.53±0.32	3
$[Ni(nap)_2(bipy)(CH_3OH)]$	12.51±0.45 / 13.61±0.23	88.82±0.60	90.65±0.82	3
$[Ni(nap)_2(phen)(H_2O)]$	15.67±0.61 / 14.48±0.34	85.74±0.21	80.12±0.75	3
$[Ni(nap)_2(bipyam)]$	8.56±0.81 / 10.21±0.63	84.59±0.92	76.39±0.20	3
$[Ni(nap)_2(Hpko)_2]$	12.28±0.34 / 13.45±0.46	97.73±0.27	92.69±0.22	3
$[Ni(nap)_2(py)_2(H_2O)_2]$	14.51±0.73 / 15.91±0.45	87.72±0.54	96.78±0.45	3

1 F. Dimiza, A.N. Papadopoulos, V. Tangoulis, V. Psycharis, C.P. Raptopoulou, D.P. Kessissoglou and G. Psomas, *J. Inorg. Biochem.*, 2012, **107**, 54-64.

2 Present work.

3 X. Totta, A.G. Hatzidimitriou, A. Papadopoulos and G. Psomas, *New J. Chem*., 2017, **41**, 4478-4492.

Table S5. Antioxidant activity (% DPPH scavenging ability (RA%) in 60 min, % superoxide radical scavenging activity (ABTS%) and competition % with DMSO for hydroxyl radical ($^{\bullet}$OH%)) of the reported metal-mefenamato complexes (metal = Mn(II), Cu(II), Co(II), Zn(II), Ni(II)).

Compound	**RA%**	**ABTS%**	**$^{\bullet}$OH %**	**Ref.**
Hmef (=mefenamic acid)	5.72±0.08 / 11.74±0.20	92.51±0.44	66.32±0.38	1
$[Mn_2(mef)_4(bipyam)_2]$, **3**	9.67±0.57 / 18.88±0.76	84.78±0.47	97.78±0.82	2
$[Mn(mef)_2(phen)(H_2O)]$, **4**	13.09±0.61 / 22.39±0.44	90.78±0.28	98.67±0.14	2
$[Mn(mef)_2(bipy)(MeOH)_2]$, **5**	9.65±0.23 / 16.58±0.33	79.06±0.31	92.47±0.66	2
$[Co(mef)_2(MeOH)_4]$	29.9 / 30.1	78.3	95.7	1
$[Co(mef)_2(bipy)(MeOH)_2]$	20.4 / 17.9	92.4	96.4	1
$[Co(mef)_2(phen)(MeOH)_2]$	32.5 / 36.8	90.4	89.3	1
$[Co(mef)_2(py)_2(MeOH)_2]$	28. 6 / 29.5	97.0	96.7	1
$[Co(mef)_2(bipyam)]$	9.32±0.78 / 12.98±0.31	76.69±0.75	95.42±0.64	3
$[Cu_2(mef)_4(H_2O)_2]$	52.4 / 54.1	75.4	67.6	4
$[Cu(mef)_2(bipy)]$	6.0 / 7.9	90.3	74.6	4
$[Cu(mef)_2(phen)]$	3.3 / 7.9	89.4	99.7	4
$[Cu(mef)_2(bipyam)]$	17.3 / 18.5	80.0	77.4	4
$[Cu(mef)_2(py)_2(MeOH)_2]$	11.8 / 21.5	98.2	75.3	4
$[Zn(mef)_2(H_2O)_4]$**, 1**	43.32±0.32 / 41.57±0.82	94.75±1.06	96.69±0.27	5
$[Zn(mef)_2(bipy)]$**, 2**	14.64±0.71 / 16.69±0.54	74.41±0.32	94.62±0.90	5
$[Zn(mef)_2(bipyam)]$**, 3**	15.22±0.48 / 18.90±0.26	90.62±0.30	82.74±0.27	5
$[Zn(mef)_2(Hpko)_2]$**, 4**	17.60±0.81 / 16.84±0.35	81.62±0.59	88.41±0.79	5
$[Zn(mef)_2(phen)(H_2O)]$**, 5**	24.17±0.46 / 28.39±0.23	77.89±0.85	89.61±0.82	5
$[Ni(mef)_2(bipy)(MeOH)_2]$	12.52±0.60 / 10.34±0.67	89.92±0.92	76.09±0.14	6
$[Ni(mef)_2(phen)(MeOH)_2]$	7.42±0.78 / 10.92±0.54	90.03±0.33	83.18±0.27	6
$[Ni(mef)_2(bipyam)]$	12.31±0.64 / 12.42±0.24	93.56±0.83	85.57±0.80	6
$[Ni(mef)_2(Hpko)_2]$	10.32±0.18 / 12.49±0.12	97.23±0.76	85.56±0.42	6
$[Ni(mef)_2(py)_2(H_2O)_2]$	12.56±0.82 / 13.03±0.68	94.76±0.12	75.28±0.64	6
$[Ni(mef)_2(MeOH)_4]$	10.49±0.74 / 12.38±0.52	89.61±0.68	78.12±0.89	6

1 F. Dimiza, A.N. Papadopoulos, V. Tangoulis, V. Psycharis, C.P. Raptopoulou, D.P. Kessissoglou and G. Psomas, *Dalton Trans.*, 2010, **39**, 4517-4528.

2 Present work.

3 S. Tsiliou, L. Kefala, A.G. Hatzidimitriou, D.P. Kessissoglou, F. Perdih, A.N. Papadopoulos, I. Turel and G. Psomas, *J. Inorg. Biochem*., 2016, **160**, 125-139.

4 F. Dimiza, S. Fountoulaki, A.N. Papadopoulos, C.A. Kontogiorgis, V. Tangoulis, C.P. Raptopoulou, V. Psycharis, A. Terzis, D.P. Kessissoglou and G. Psomas, *Dalton Trans.*, 2011, **40**, 8555-8568.

5 A. Tarushi, Z. Karaflou, J. Kljun, I. Turel, G. Psomas, A.N. Papadopoulos and D.P. Kessissoglou, *J. Inorg. Biochem.*, 2013, **128**, 85-96.

6 X. Totta, A.A. Papadopoulou, A.G. Hatzidimitriou, A. Papadopoulos and G. Psomas, *J. Inorg. Biochem*., 2015, **145**, 79-93.

Table S6. % DPPH scavenging ability (RA%, for 0.1 mM), % superoxide radical scavenging activity (ABTS%, for 0.1 mM) and competition % with DMSO for hydroxyl radical (˙OH%, for 0.1 mM) for the reported Mn(II)-NSAID complexes (NSAID = naproxen, mefenamato, tolfenamato, diclofenac).

Compound	**RA%, 20 min / 60 min**	**ABTS%**	**˙OH%**	**Ref.**
Hnap (=naproxen)	8.03±0.32 / 8.43±0.20	87.51±0.17	89.55±0.44	1
$[Mn(nap)_2(py)_2(H_2O)_2]$, **1**	13.58±076 / 16.76±0.34	94.78±0.36	98.31±0.67	2
$[Mn(nap)_2(phen)(H_2O)]$, **2**	14.67±0.37 / 16.06±0.62	96.67±0.68	97.42±0.83	2
Hmef (=mefenamic acid)	5.72±0.08 / 11.74±0.20	66.32±0.38	92.51±0.44	3
$[Mn_2(mef)_4(bipyam)_2]$, **3**	9.67±0.57 / 18.88±0.76	84.78±0.47	97.78±0.82	2
$[Mn(mef)_2(phen)(H_2O)]$, **4**	13.09±0.61 / 22.39±0.44	90.78±0.28	98.67±0.14	2
$[Mn(mef)_2(bipy)(MeOH)_2]$, **5**	9.65±0.23 / 16.58±0.33	79.06±0.31	92.47±0.66	2
Htolf (=tolfenamic acid)	14.57±0.62 / 17.86±0.54	59.43±0.33	75.46±0.44	4
$[Mn(tolf)_{2(}phen)(H_2O)]$	26.42±0.54) / 28.35±0.54	78.44±0.38	91.47±0.51	4
$[Mn_2(tolf)_4(py)_4(H_2O)]$	16.86±0.89 / 15.97±0.54	72.83±0.45	86.53±0.38	4
$[Mn_2(tolf)_4(bipyam)_2]$	16.73±0.51 / 19.46±0.54	68.47±0.21	87.02±0.60	4
$[Mn(tolf)_2(DMF)_2]_n$	19.66±0.59 / 19.89±0.55	71.38±0.41	85.95±0.40	4
Na-dicl (sodium diclofenac)	18.26±0.60 / 17.43±0.23	76.35±0.75	75.46±0.44	5
$[Mn(dicl)(bipy)(H_2O)_2](dicl)$	24.86±0.29 / 29.31±0.64	71.54±0.83	89.04±0.92	6
$[Mn(dicl)_2(py)_2(H_2O)_2]$	21.56±0.48 / 21.54±0.28	84.72±1.09	81.34±0.84	6
$[Mn(dicl)_2(bipyam)]$	22.48±0.44 / 21.54±0.28	70.34±0.60	91.37±0.54	5
$[Mn_3(dicl)_6(phen)_2(MeOH)]$	34.62±0.81 / 37.81(±0.63	89.58±0.93	94.58±1.14	5

1 F. Dimiza, A.N. Papadopoulos, V. Tangoulis, V. Psycharis, C.P. Raptopoulou, D.P. Kessissoglou and G. Psomas, *J. Inorg. Biochem.*, 2012, **107**, 54-64.

2 Present work.

3 F. Dimiza, A.N. Papadopoulos, V. Tangoulis, V. Psycharis, C.P. Raptopoulou, D.P. Kessissoglou and G. Psomas, *Dalton Trans.*, 2010, **39**, 4517-4528.

4 M. Zampakou, N. Rizeq, V. Tangoulis, A. N. Papadopoulos, F. Perdih, I. Turel and G. Psomas, *Inorg. Chem.*, 2014, **53**, 2040-2052.

5 M. Zampakou, V. Tangoulis, C.P. Raptopoulou, V. Psycharis, A.N. Papadopoulos and G. Psomas, *Eur. J. Inorg. Chem.*, 2015, 2285-2294.

6 M. Zampakou, A.G. Hatzidimitriou, A.N. Papadopoulos and G. Psomas, *J. Coord. Chem.*, 2015, **68**, 4355-4372.

Table S7. The BSA and HSA constants and parameters derived for Hmef, Hnap and complexes **1-5.**

Compound	**Ksv (M^{-1})**	**k_q ($M^{-1}s^{-1}$)**	**K(M^{-1})**	**n**
BSA				
Hnap [1]	$1.18(\pm0.06)\times10^{4}$	$1.18(\pm0.06)\times10^{12}$	$5.35(\pm0.42)\times10^{3}$	2.03
Hmef [2]	$2.78(\pm0.20)\times10^{5}$	$2.78(\pm0.20)\times10^{13}$	$1.35(\pm0.22)\times10^{5}$	1.20
$[Mn(nap)_2(py)_2(H_2O)_2]$, **1**	$1.35(\pm0.10)\times10^{4}$	$1.35(\pm0.10)\times10^{12}$	$9.99(\pm0.45)\times10^{5}$	0.34
$[Mn(nap)_2(phen)(H_2O)]$, **2**	$2.39(\pm0.07)\times10^{4}$	$2.39(\pm0.07)\times10^{12}$	$1.61(\pm0.25)\times10^{4}$	1.30
$[Mn_2(mef)_4(bipyam)_2]$, **3**	$3.24(\pm0.22)\times10^{6}$	$3.24(\pm0.22)\times10^{14}$	$1.09(\pm0.04)\times10^{6}$	1.05
$[Mn(mef)_2(phen)(H_2O)]$, **4**	$1.32(\pm0.04)\times10^{5}$	$1.32(\pm0.04)\times10^{13}$	$2.17(\pm0.07)\times10^{5}$	0.89
$[Mn(mef)_2(bipy)(MeOH)_2]$, **5**	$3.61(\pm0.32)\times10^{5}$	$3.61(\pm0.32)\times10^{13}$	$1.59(\pm0.08)\times10^{6}$	0.89
HSA				
Hnap [1]	$1.24(\pm0.09)\times10^{4}$	$1.24(\pm0.09)\times10^{12}$	$3.27(\pm0.30)\times10^{4}$	0.43
Hmef [2]	$7.13(\pm0.34)\times10^{4}$	$7.13(\pm0.34)\times10^{12}$	$1.32(\pm0.15)\times10^{5}$	0.82
$[Mn(nap)_2(py)_2(H_2O)_2]$, **1**	$2.25(\pm0.12)\times10^{4}$	$2.25(\pm0.12)\times10^{12}$	$6.50(\pm0.30)\times10^{4}$	0.57
$[Mn(nap)_2(phen)(H_2O)]$, **2**	$9.06(\pm0.26)\times10^{4}$	$9.06(\pm0.26)\times10^{12}$	$3.30(\pm0.28)\times10^{5}$	0.61
$[Mn_2(mef)_4(bipyam)_2]$, **3**	$4.98(\pm0.19)\times10^{5}$	$4.98(\pm0.19)\times10^{13}$	$6.78(\pm0.35)\times10^{5}$	0.95
$[Mn(mef)_2(phen)(H_2O)]$, **4**	$9.19(\pm0.34)\times10^{4}$	$9.19(\pm0.34)\times10^{12}$	$2.34(\pm0.09)\times10^{5}$	0.71
$[Mn(mef)_2(bipy)(MeOH)_2]$, **5**	$5.98(\pm0.38)\times10^{4}$	$5.98(\pm0.38)\times10^{12}$	$3.29(\pm0.12)\times10^{5}$	0.65

1 F. Dimiza, A.N. Papadopoulos, V. Tangoulis, V. Psycharis, C.P. Raptopoulou, D.P. Kessissoglou and G. Psomas, *J. Inorg. Biochem.*, 2012, **107**, 54-64.

2 F. Dimiza, A.N. Papadopoulos, V. Tangoulis, V. Psycharis, C.P. Raptopoulou, D.P. Kessissoglou and G. Psomas, *Dalton Trans.*, 2010, **39**, 4517-4528.

Table S8. DNA-, BSA- and HSA-binding constants for the reported metal-naproxen complexes (metal = Mn(II), Cu(II), Co(II), Ni(II)).

Compound	**K_b (M^{-1})**	**$K_{(BSA)}$ (M^{-1})**	**$K_{(HSA)}$ (M^{-1})**	**Reference**
Hnap (naproxen)	2.67×10^4	$5.35x10^3$	3.27×10^4	1
$[Mn(nap)_2(py)_2(H_2O)_2]$, **1**	2.29×10^4	9.99×10^5	6.50×10^4	2
$[Mn(nap)_2(phen)(H_2O)]$, **2**	6.40×10^6	1.61×10^4	3.30×10^5	2
$[Cu(nap)_2(bipy)]$	3.86×10^4	1.20×10^4	3.20×10^4	1
$[Cu(nap)_2(phen)]$	9.20×10^3	1.90×10^4	7.69×10^4	1
$[Cu_2(nap)_4(H_2O)_2]$	2.27×10^4	6.61×10^4	7.83×10^4	1
$[Cu(nap)_2(py)_2(H_2O)]$	8.97×10^3	2.55×10^4	9.55×10^3	1
$[Co(nap)_2(MeOH)_4]$	3.15×10^4	1.25×10^5	3.20×10^4	1
$[Co(nap)_2(py)_2(H_2O)_2]$	2.29×10^4	2.64×10^4	2.69×10^4	1
$[Co(nap)_2(phen)(H_2O)_2]$	2.76×10^4	1.07×10^5	1.58×10^4	1
$[Co(nap)_2(bipy)(H_2O)_2]$	3.58×10^4	3.06×10^4	2.19×10^4	1
$[Ni(nap)_2(MeOH)_4]$	1.47×10^5	4.51×10^4	1.35×10^4	3
$[Ni(nap)_2(bipy)(MeOH)]$	5.96×10^5	3.25×10^5	1.93×10^5	3
$[Ni(nap)_2(phen)(H_2O)]$	1.54×10^5	4.18×10^5	2.73×10^4	3
$[Ni(nap)_2(bipyam)]$	2.91×10^5	4.59×10^4	1.88×10^5	3
$[Ni(nap)_2(Hpko)_2]$	8.01×10^5	1.08×10^5	3.02×10^4	3
$[Ni(nap)_2(py)_2(H_2O)_2]$	6.14×10^5	7.44×10^3	4.05×10^4	3

1 F. Dimiza, A.N. Papadopoulos, V. Tangoulis, V. Psycharis, C.P. Raptopoulou, D.P. Kessissoglou and G. Psomas, *J. Inorg. Biochem.*, 2012, **107**, 54-64.

2 Present work.

3 X. Totta, A.G. Hatzidimitriou, A. Papadopoulos and G. Psomas, *New J. Chem.*, 2017, **41**, 4478-4492.

Table S9. DNA-, BSA- and HSA-binding constants for the reported metal-mefenamato complexes (metal = Mn(II), Cu(II), Co(II), Zn(II), Ni(II)).

Compound	**K_b (M^{-1})**	**$K_{(BSA)}$ (M^{-1})**	**$K_{(HSA)}$ (M^{-1})**	**Reference**
Hmef (=mefenamic acid)	1.05×10^5	1.35×10^5	1.32×10^5	1
$[Mn_2(mef)_4(bipyam)_2]$, **3**	1.13×10^6	1.09×10^6	6.78×10^5	2
$[Mn(mef)_2(phen)(H_2O)]$, **4**	4.47×10^6	2.17×10^5	2.34×10^5	2
$[Mn(mef)_2(bipy)(MeOH)_2]$, **5**	4.38×10^6	1.59×10^6	3.29×10^5	2
$[Co(mef)_2(MeOH)_4]$	5.82×10^4	2.22×10^5	1.46×10^5	1
$[Co(mef)_2(bipy)(MeOH)_2]$	4.59×10^4	2.38×10^5	1.34×10^5	1
$[Co(mef)_2(phen)(MeOH)_2]$	3.02×10^4	3.66×10^5	1.49×10^5	1
$[Co(mef)_2(py)_2(MeOH)_2]$	3.22×10^5	2.37×10^5	2.43×10^5	1
$[Co(mef)_2(bipyam)]$	6.70×10^4	2.77×10^5	6.10×10^5	3
$[Cu_2(mef)_4(H_2O)_2]$	7.59×10^5	2.47×10^5	1.69×10^5	4
$[Cu(mef)_2(bipy)]$	9.03×10^4	1.58×10^5	1.37×10^5	4
$[Cu(mef)_2(phen)]$	6.95×10^5	2.59×10^5	1.61×10^5	4
$[Cu(mef)_2(bipyam)]$	2.20×10^5	1.28×10^6	2.52×10^5	4
$[Cu(mef)_2(py)_2(MeOH)_2]$	6.93×10^4	2.33×10^5	2.21×10^5	4
$[Zn(mef)_2(H_2O)_4]$**, 1**	6.81×10^5	5.05×10^7	5.29×10^6	5
$[Zn(mef)_2(bipy)]$**, 2**	5.37×10^5	1.05×10^6	3.43×10^5	5
$[Zn(mef)_2(bipyam)]$**, 3**	5.82×10^5	8.76×10^5	6.19×10^5	5
$[Zn(mef)_2(Hpko)_2]$**, 4**	1.93×10^7	4.78×10^5	1.59×10^5	5
$[Zn(mef)_2(phen)(H_2O)]$**, 5**	3.91×10^4	4.80×10^5	1.51×10^5	5
$[Ni(mef)_2(bipy)(MeOH)_2]$	1.20×10^5	3.23×10^5	2.44×10^5	6
$[Ni(mef)_2(phen)(MeOH)_2]$	8.26×10^4	3.10×10^5	2.23×10^5	6
$[Ni(mef)_2(bipyam)]$	1.46×10^5	2.33×10^5	2.03×10^5	6
$[Ni(mef)_2(Hpko)_2]$	1.15×10^6	1.35×10^5	3.42×10^5	6
$[Ni(mef)_2(py)_2(H_2O)_2]$	1.19×10^5	3.22×10^5	3.85×10^5	6
$[Ni(mef)_2(MeOH)_4]$	2.62×10^5	2.11×10^5	3.00×10^5	6

1 F. Dimiza, A.N. Papadopoulos, V. Tangoulis, V. Psycharis, C.P. Raptopoulou, D.P. Kessissoglou and G. Psomas, *Dalton Trans.*, 2010, **39**, 4517-4528.

2 Present work.

3 S. Tsiliou, L. Kefala, A.G. Hatzidimitriou, D.P. Kessissoglou, F. Perdih, A.N. Papadopoulos, I. Turel and G. Psomas, *J. Inorg. Biochem*., 2016, **160**, 125-139.

4 F. Dimiza, S. Fountoulaki, A.N. Papadopoulos, C.A. Kontogiorgis, V. Tangoulis, C.P. Raptopoulou, V. Psycharis, A. Terzis, D.P. Kessissoglou and G. Psomas, *Dalton Trans.*, 2011, **40**, 8555-8568.

5 A. Tarushi, Z. Karaflou, J. Kljun, I. Turel, G. Psomas, A.N. Papadopoulos and D.P. Kessissoglou, *J. Inorg. Biochem.*, 2013, **128**, 85-96.

6 X. Totta, A.A. Papadopoulou, A.G. Hatzidimitriou, A. Papadopoulos and G. Psomas, *J. Inorg. Biochem*., 2015, **145**, 79-93.

Table S10. DNA-, BSA- and HSA-binding constants for the reported manganese(II)-NSAID complexes (NSAID = naproxen, mefenamato, tolfenamato, diclofenac, niflumato).

Compound	**K_b (M^{-1})**	**$K_{(BSA)}$ (M^{-1})**	**$K_{(HSA)}$ (M^{-1})**	**Reference**
Hnap (=naproxen)	2.67×10^4	5.35×10^3	3.27×10^4	1
$[Mn(nap)_2(py)_2(H_2O)_2]$, **1**	2.29×10^4	9.99×10^5	6.50×10^4	2
$[Mn(nap)_2(phen)(H_2O)]$, **2**	6.40×10^6	1.61×10^4	3.30×10^5	2
Hmef (=mefenamic acid)	1.05×10^5	1.35×10^5	1.32×10^5	3
$[Mn_2(mef)_4(bipyam)_2]$, **3**	1.13×10^6	1.09×10^6	6.78×10^5	2
$[Mn(mef)_2(phen)(H_2O)]$, **4**	4.47×10^6	2.17×10^5	2.34×10^5	2
$[Mn(mef)_2(bipy)(MeOH)_2]$, **5**	4.38×10^6	1.59×10^6	3.29×10^5	2
Htolf (=tolfenamic acid)	5.00×10^4	1.60×10^5	3.12×10^5	4
$[Mn(tolf)_{2(}phen)(H_2O)]$	2.62×10^4	1.86×10^6	3.56×10^5	4
$[Mn_2(tolf)_4(py)_4(H_2O)]$	1.35×10^5	4.32×10^6	6.66×10^5	4
$[Mn_2(tolf)_4(bipyam)_2]$	2.65×10^5	4.26×10^6	9.04×10^5	4
$[Mn(tolf)_2(DMF)_2]_n$	5.21×10^5	4.29×10^5	5.88×10^5	4
Nadicl (=sodium diclofenac)	3.16×10^4	3.55×10^5	1.63×10^5	5
$[Mn(dicl)(bipy)(H_2O)_2](dicl)$	3.60×10^4	3.18×10^5	2.53×10^5	6
$[Mn(dicl)_2(py)_2(H_2O)_2]$	3.59×10^4	2.30×10^5	2.70×10^4	6
$[Mn(dicl)_2(bipyam)]$	1.24×10^5	3.14×10^6	3.89×10^5	5
$[Mn_3(dicl)_6(phen)_2(MeOH)]$	4.56×10^5	1.15×10^6	1.86×10^5	5
Hnif (=niflumic acid)	7.60×10^5	1.18×10^6	4.14×10^5	7
$[Mn(nif)_2(H_2O)_4]$	8.67×10^5	2.89×10^6	3.80×10^5	7

1 F. Dimiza, A.N. Papadopoulos, V. Tangoulis, V. Psycharis, C.P. Raptopoulou, D.P. Kessissoglou and G. Psomas, *J. Inorg. Biochem.*, 2012, **107**, 54-64.

2 Present work.

3 F. Dimiza, A.N. Papadopoulos, V. Tangoulis, V. Psycharis, C.P. Raptopoulou, D.P. Kessissoglou and G. Psomas, *Dalton Trans.*, 2010, **39**, 4517-4528.

4 M. Zampakou, N. Rizeq, V. Tangoulis, A. N. Papadopoulos, F. Perdih, I. Turel and G. Psomas, *Inorg. Chem.*, 2014, **53**, 2040-2052.

5 M. Zampakou, V. Tangoulis, C.P. Raptopoulou, V. Psycharis, A.N. Papadopoulos and G. Psomas, *Eur. J. Inorg. Chem.*, 2015, 2285-2294.

6 M. Zampakou, A.G. Hatzidimitriou, A.N. Papadopoulos and G. Psomas, *J. Coord. Chem.*, 2015, **68**, 4355-4372.

7 P. Tsiliki, F. Perdih, I. Turel and G. Psomas, *Polyhedron*, 2013, **53**, 215-222.

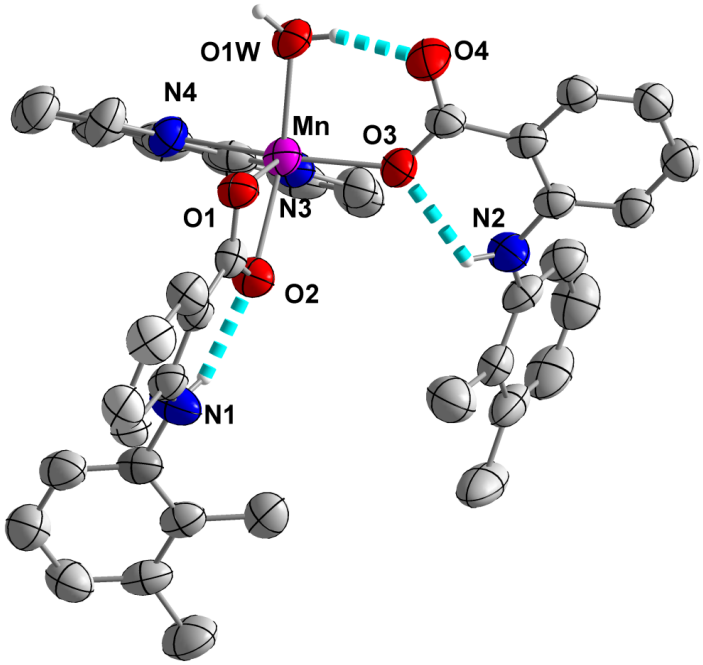

Figure S1. Ortep plot of **4** with only the heteroatoms labeled. The thermal ellipsoids are shown at a 50% probability level. Dashed cyan lines indicate intramolecular hydrogen bonds.

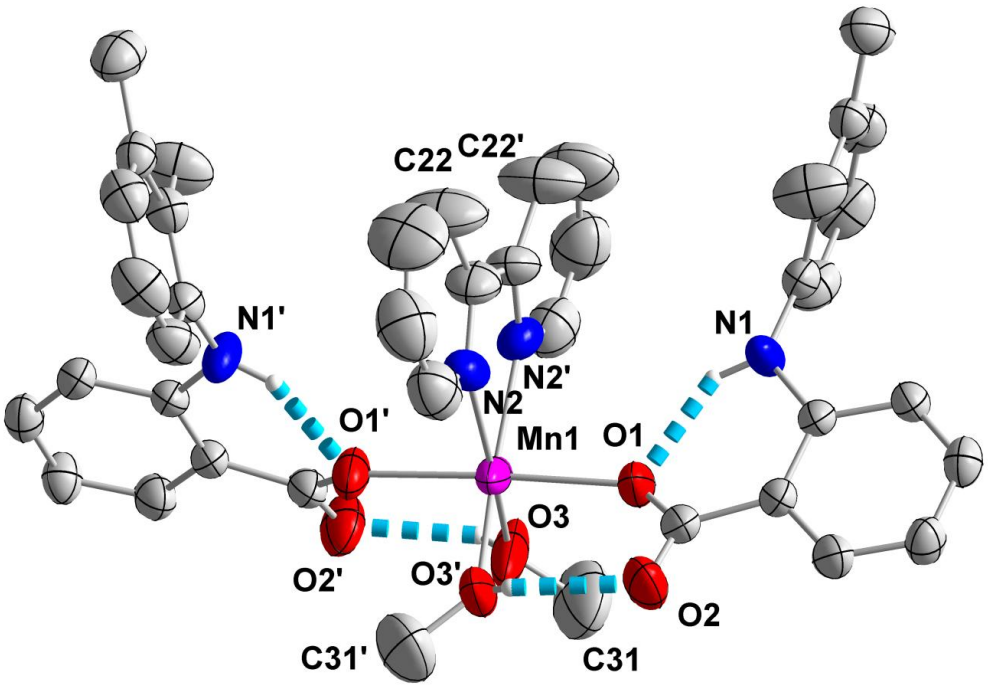

Figure S2. Ortep plot of **5** with only the heteroatoms labeled. The thermal ellipsoids are shown at a 50% probability level. Dashed cyan lines indicate intraligand and intramolecular hydrogen bonds. Symmetry code: (′): 2-x, y, 1-z.

(A)

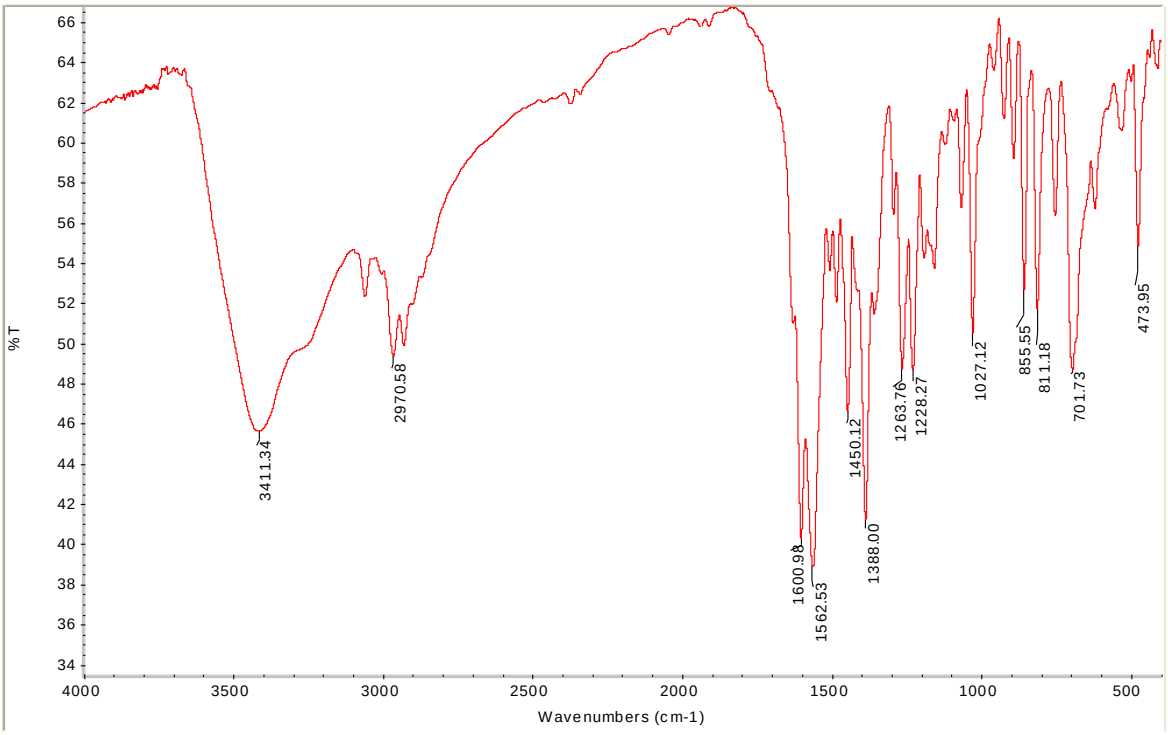
%T
Wavenumbers (cm-1)
3411.34
2970.58
1600.98
1562.53
1450.12
1388.00
1263.76
1228.27
1027.12
855.55
811.18
701.73
473.95

(B)

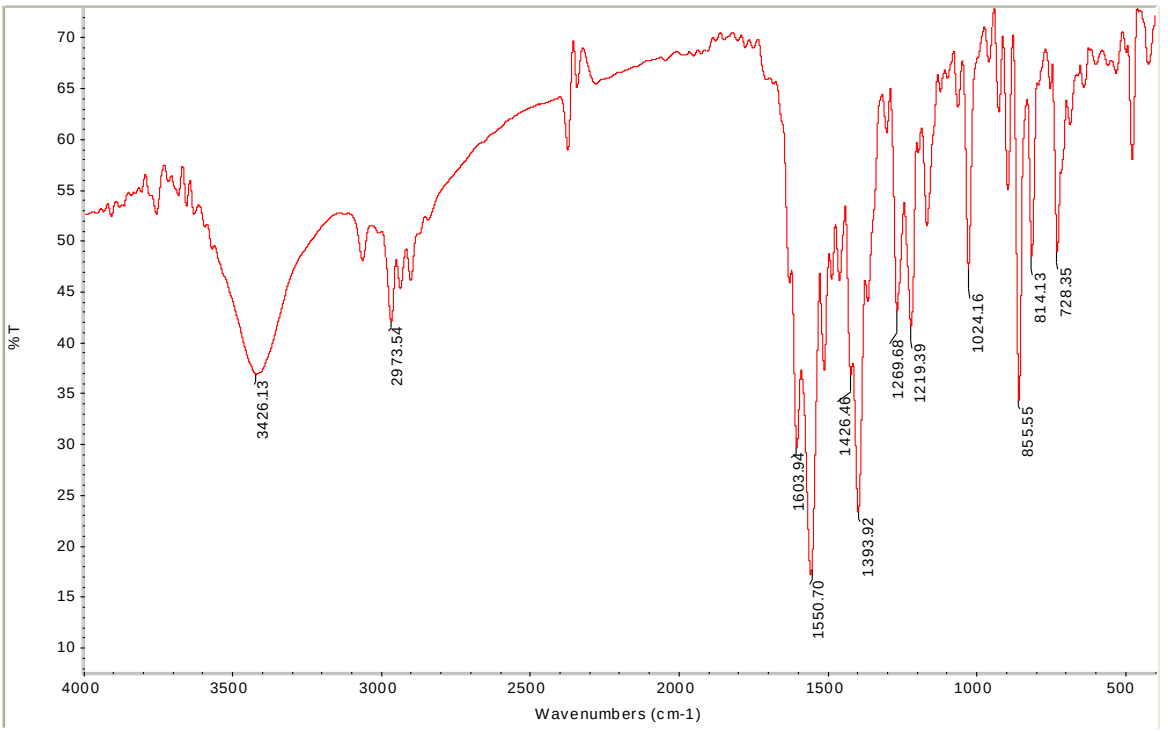
%T
Wavenumbers (cm-1)
3426.13
2973.54
1603.94
1550.70
1426.46
1393.92
1269.68
1219.39
1024.16
855.55
814.13
728.35

(C)

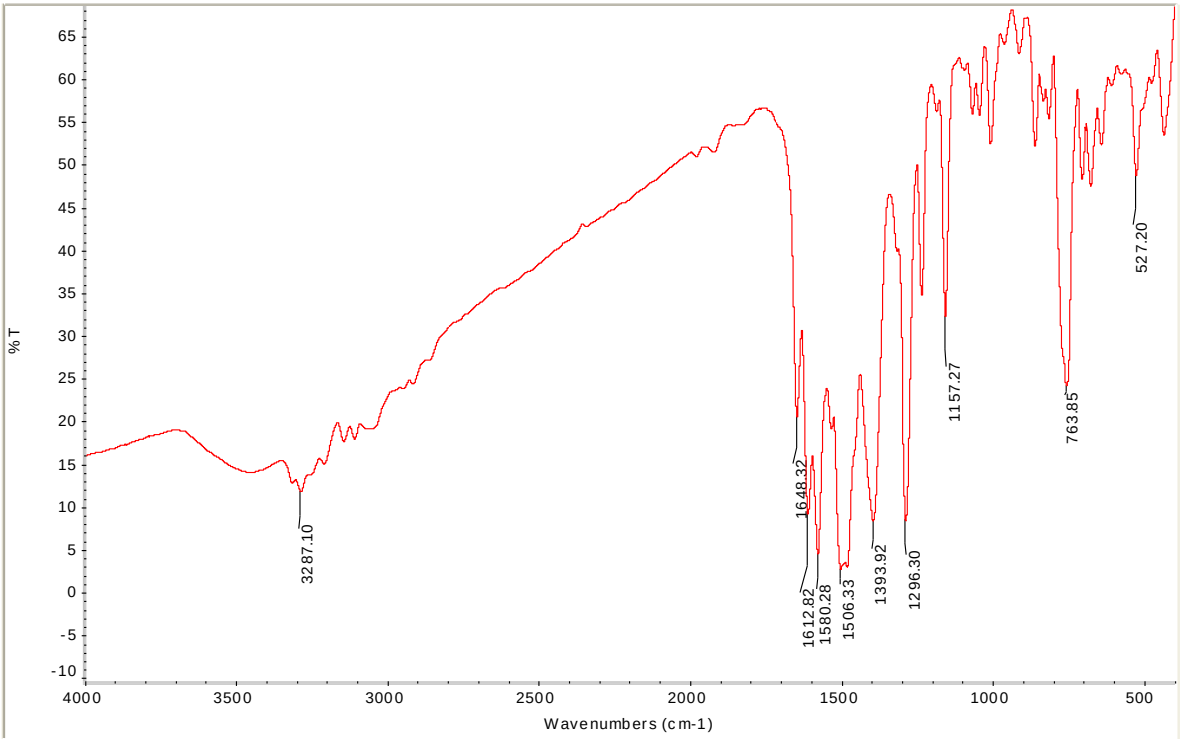
%T
Wavenumbers (cm-1)
3287.10
1648.32
1612.82
1580.28
1506.33
1393.92
1296.30
1157.27
763.85
527.20

(D)

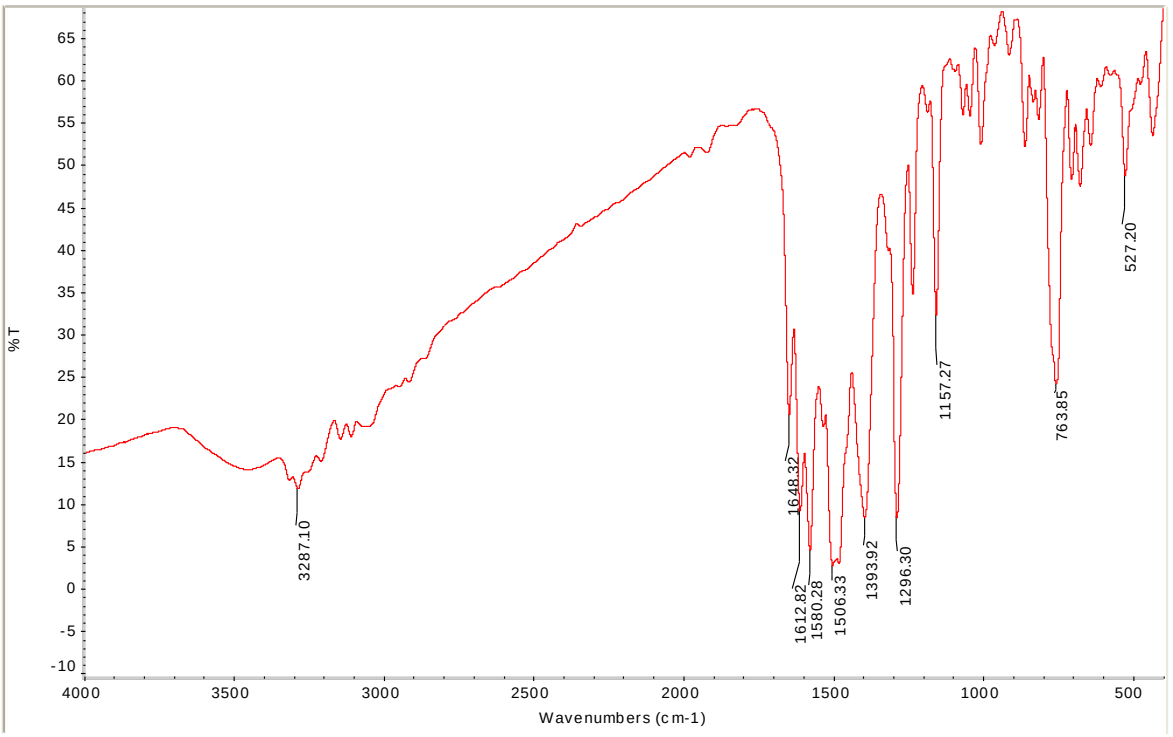
%T
Wavenumbers (cm-1)
3287.10
1648.32
1612.82
1580.28
1506.33
1393.92
1296.30
1157.27
763.85
527.20

(E)

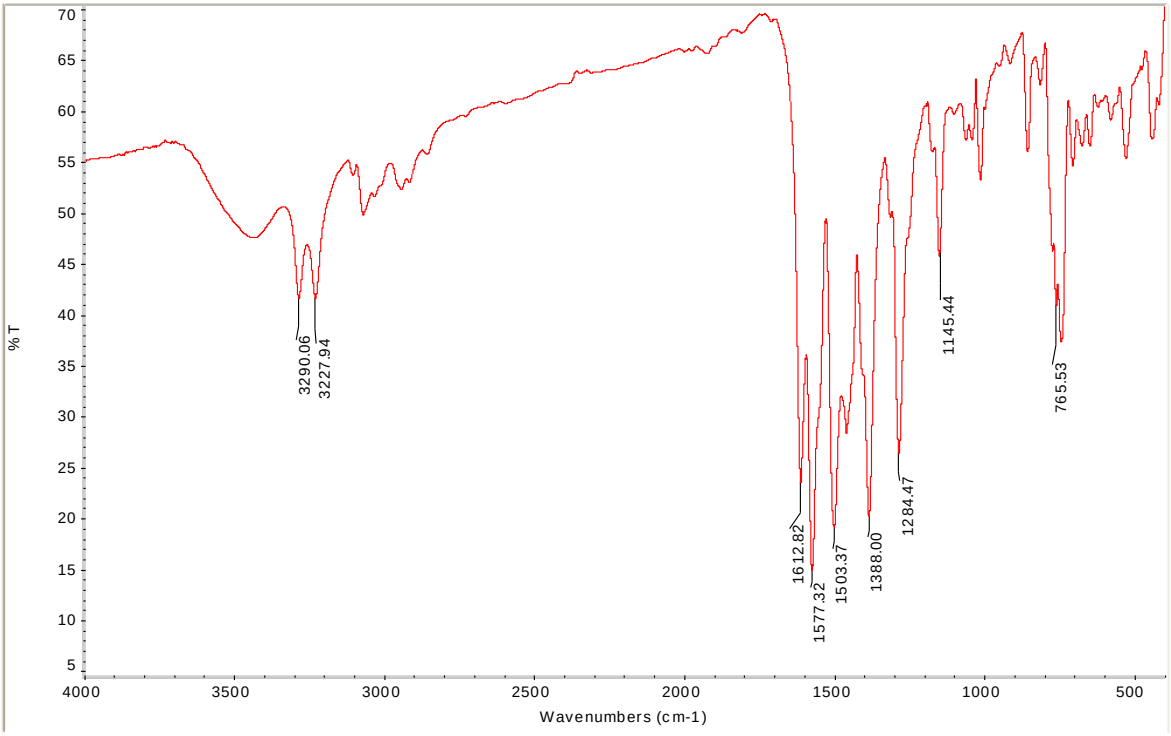

Figure S3. IR spectra (in KBr) of complex (A) **1**, (B) **2**, (C) **3**, (D) **4** and (E) **5.**

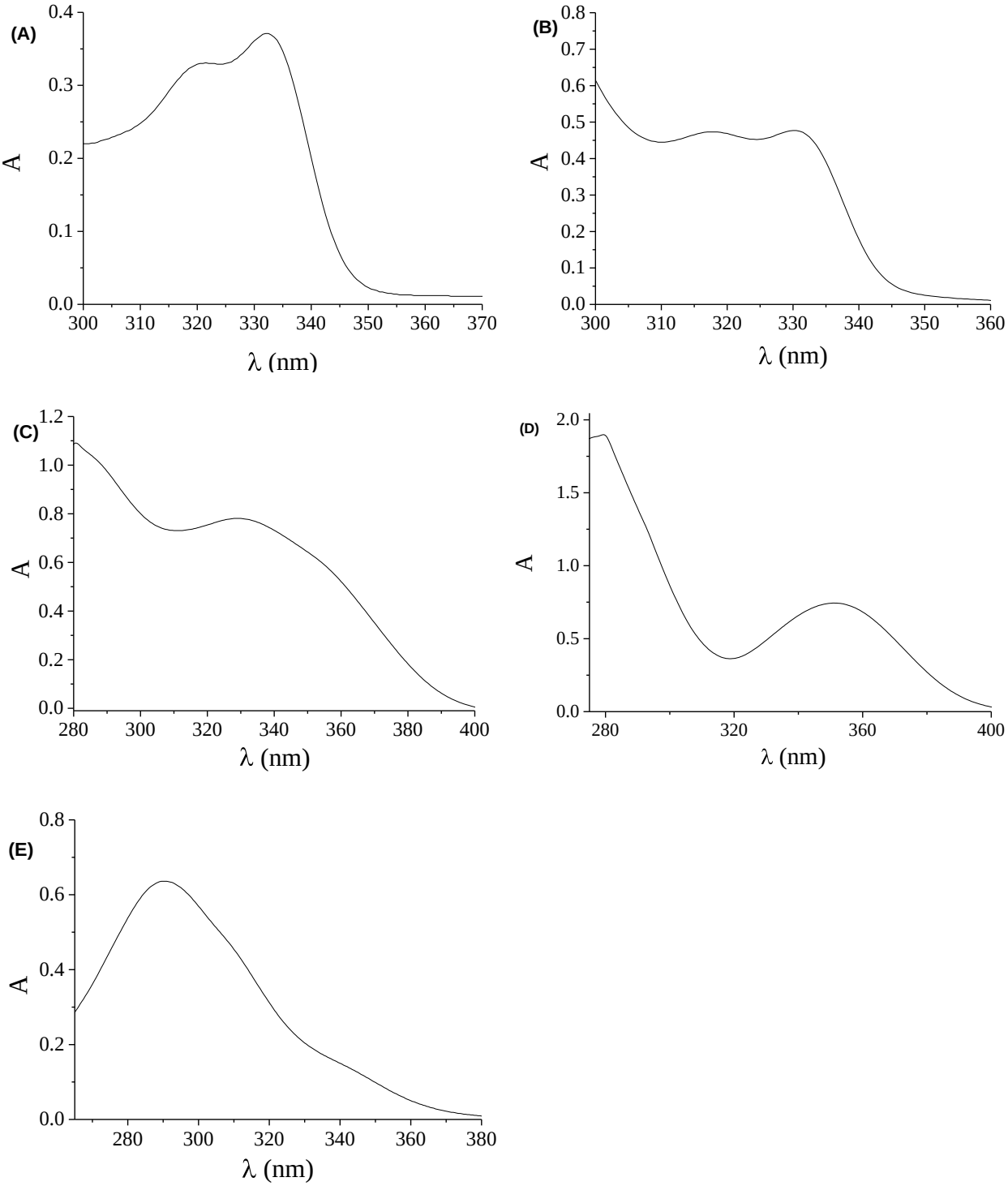

Figure S4. UV-vis spectra of DMSO solution of complex (A) **1** (5×10^{-5} M), (B) **2** (5×10^{-5} M), (C) **3** (1×10^{-5} M), (D) **4** (2.5×10^{-5} M) and (E) **5** (2×10^{-5} M).

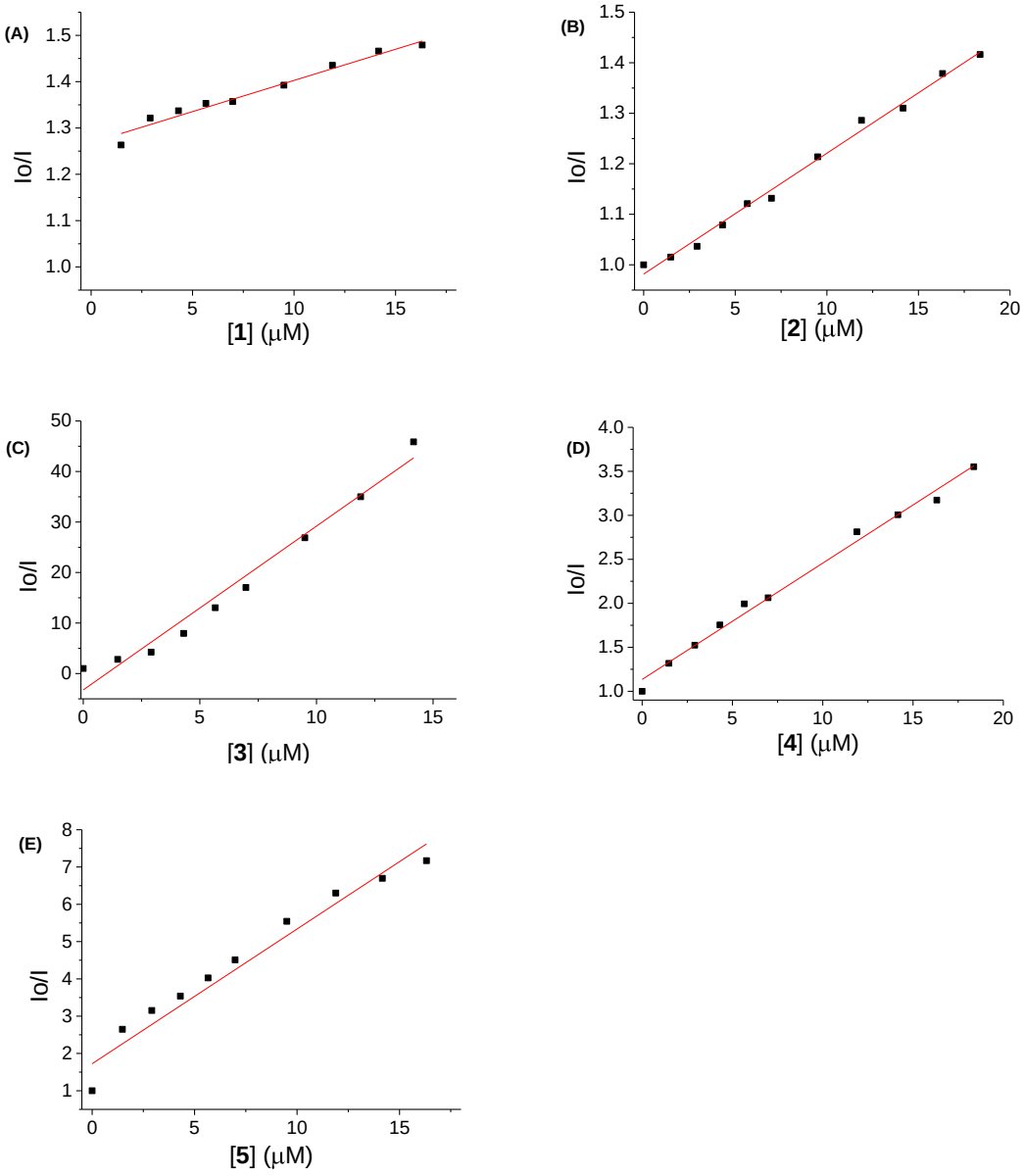

Figure S5. Stern-Volmer quenching plots of BSA for complexes (A)-(E) **1**-**5**, respectively.

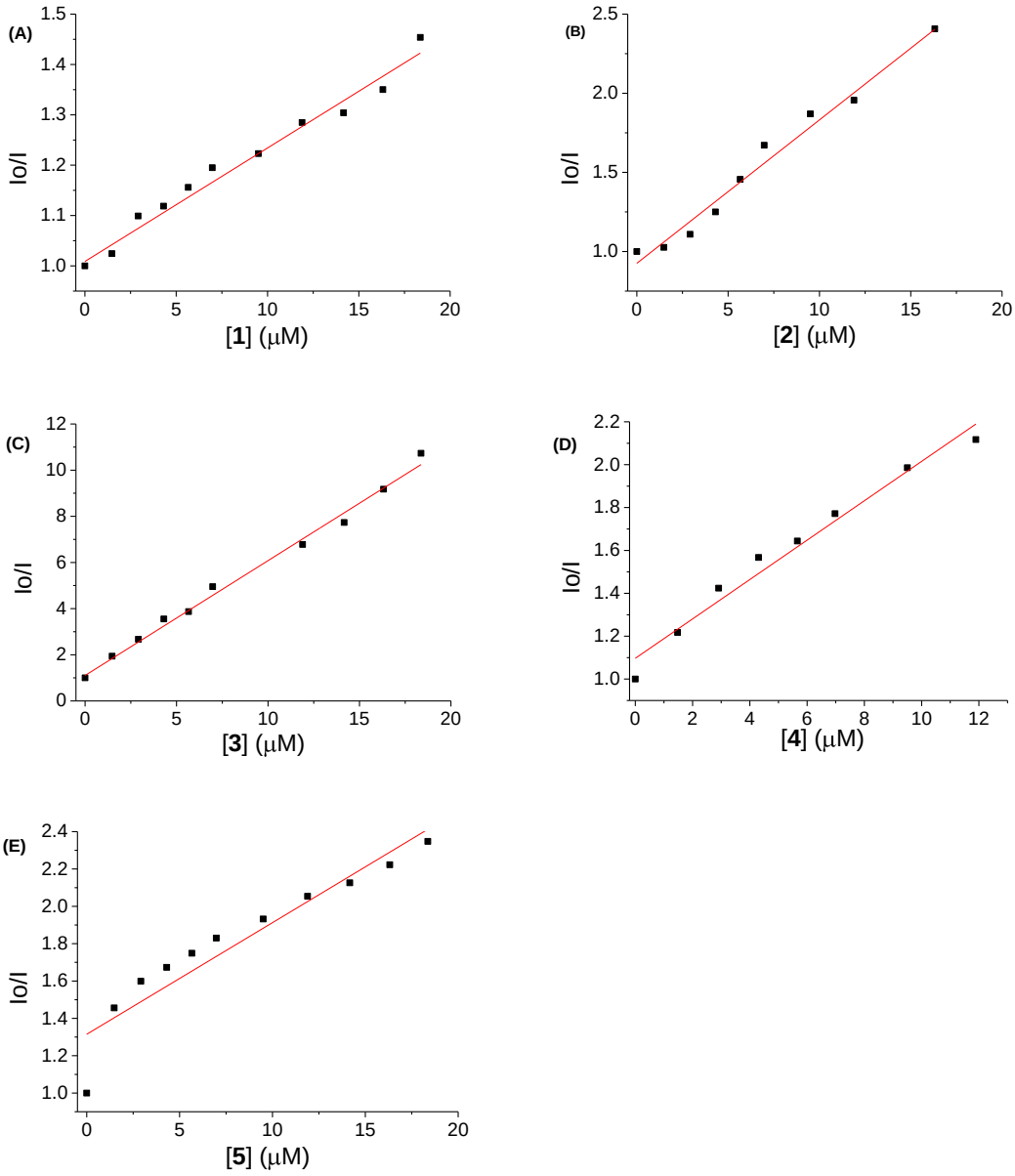

Figure S6. Stern-Volmer quenching plots of HSA for complexes (A)-(E) **1**-**5**, respectively.

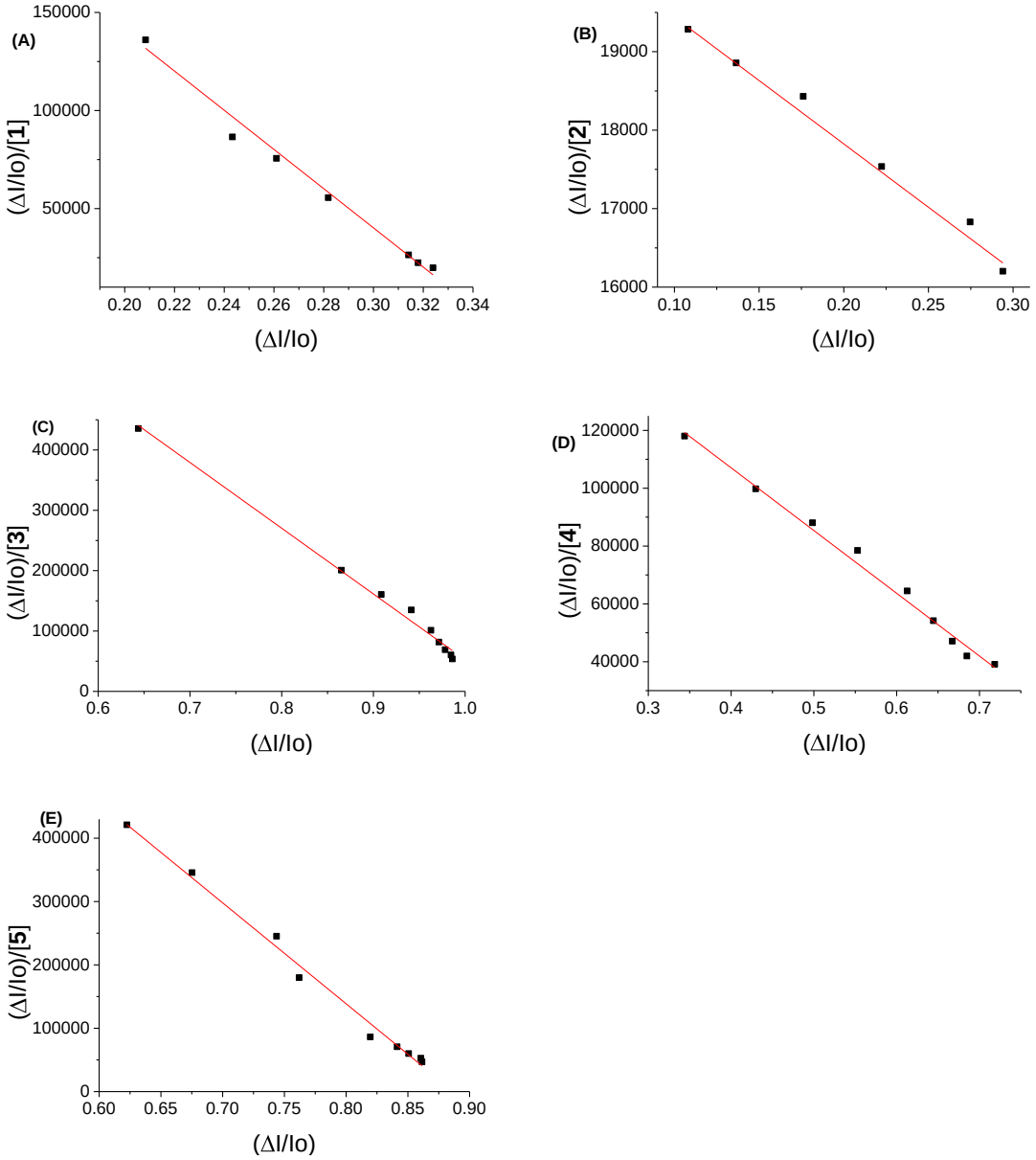

Figure S7. Scatchard plots of BSA for complexes (A)-(E) **1**-**5**, respectively.

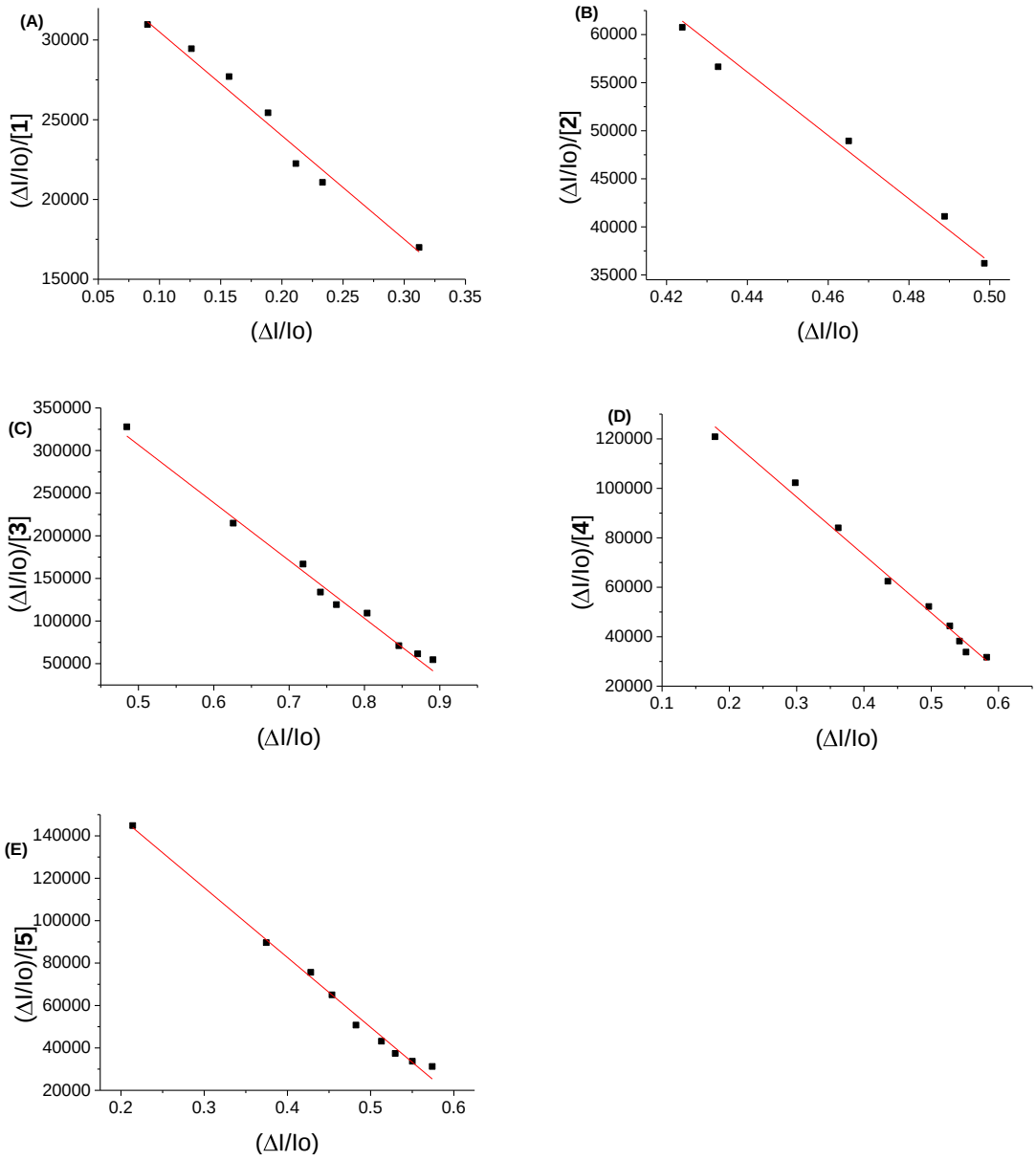

Figure S8. Scatchard plots of HSA for complexes (A)-(E) **1-5**, respectively.

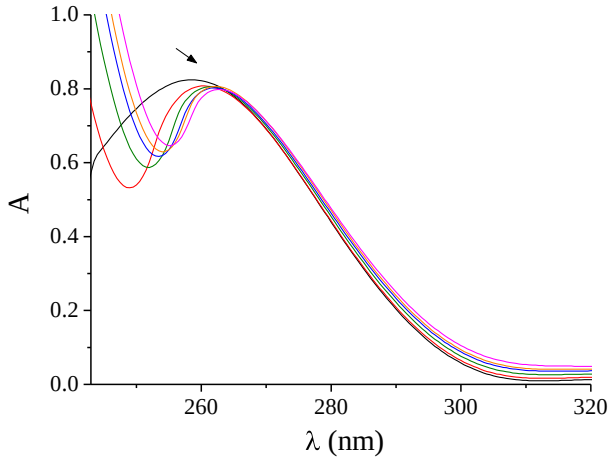

Figure S9. UV-vis spectra of a buffer solution (15 mM trisodium citrate and 150 mM NaCl at pH 7.0) of CT DNA (1.25×10^{-4} M) in the presence of increasing amounts of complex **3**. The arrow shows the changes upon increasing amounts of the complex.

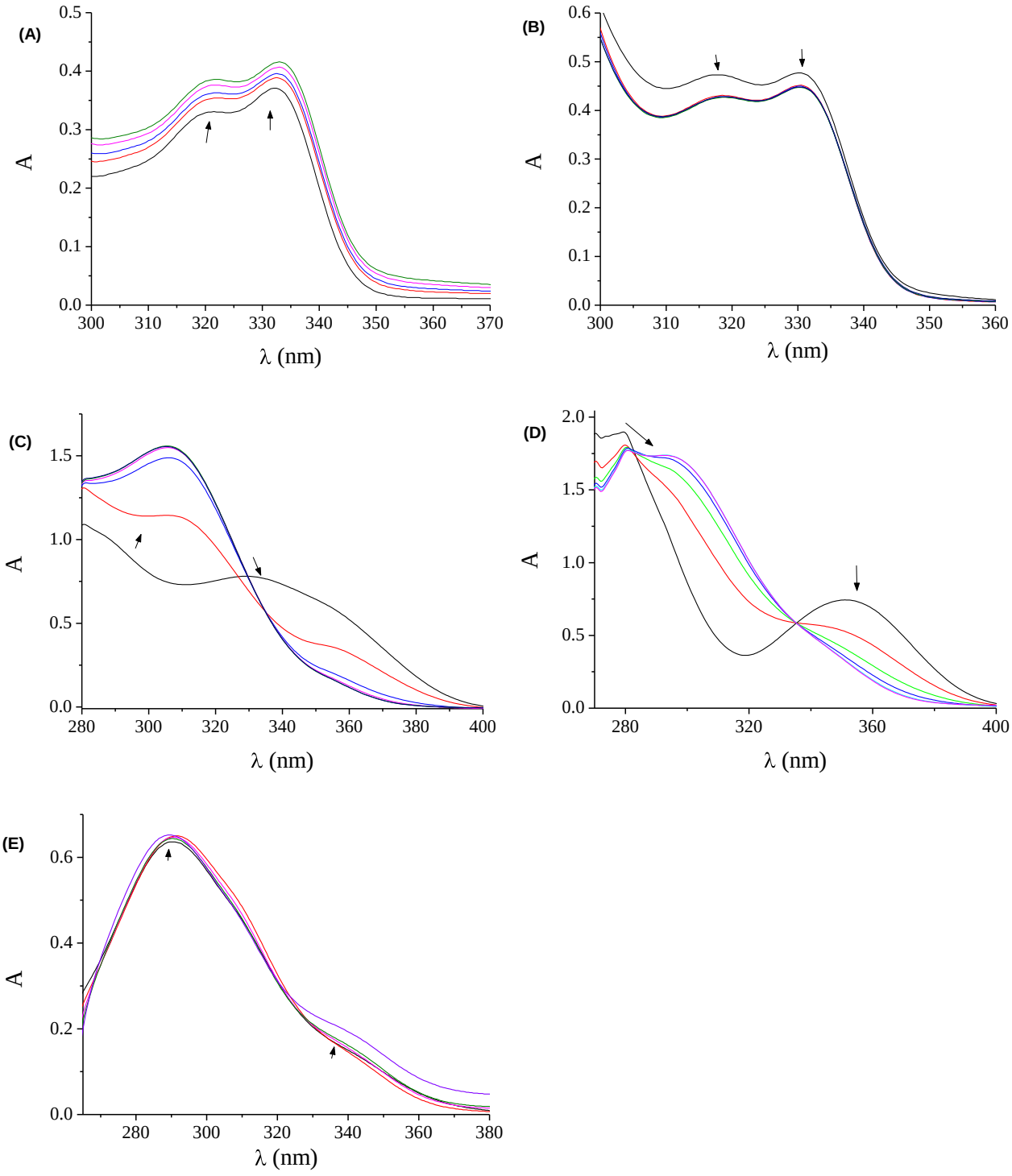

Figure S10. UV-vis spectra of DMSO solution of complex (A) **1** (5×10^{-5} M), (B) **2** (5×10^{-5} M), (C) **3** (1×10^{-5} M), (D) **4** (2.5×10^{-5} M) and (E) **5** (2×10^{-5} M) in the presence of increasing amounts of CT DNA. The arrows show the changes upon addition of increasing amounts of CT DNA.

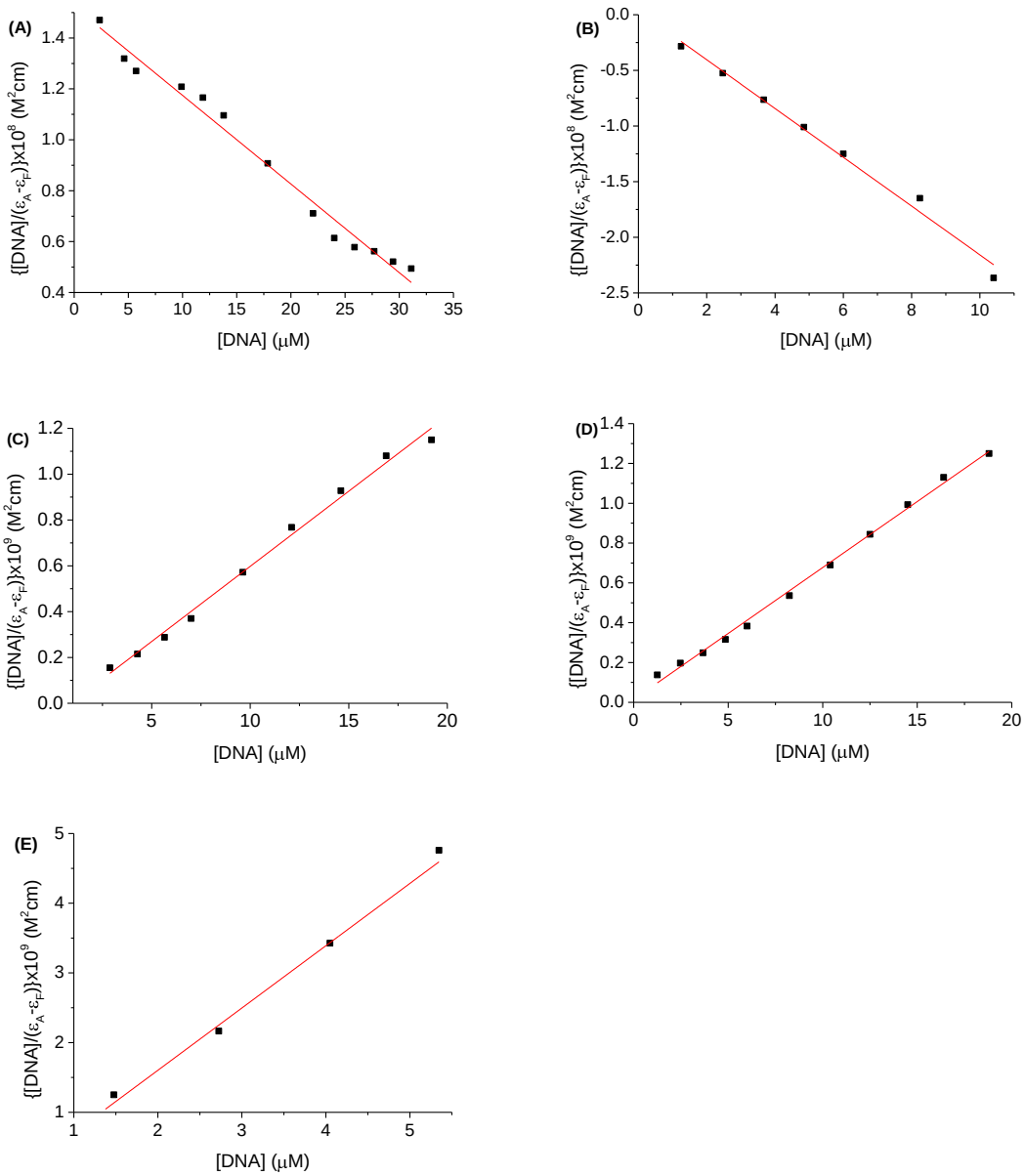

Figure S11. Plot of [DNA]/(ε_A-ε_f) *versus* [DNA] for complexes (A)-(E) **1**-**5**, respectively.

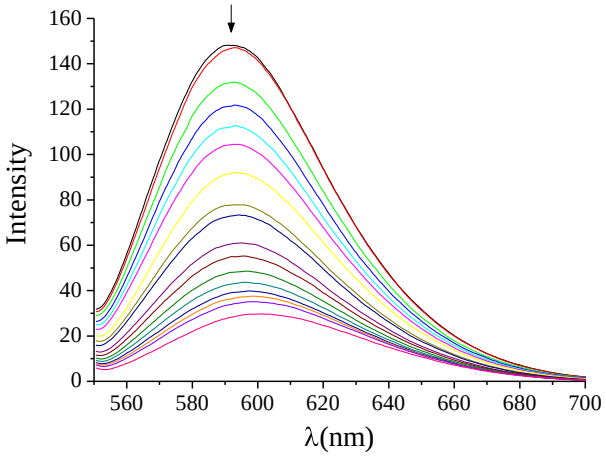

Figure S12. Fluorescence emission spectra (λ_{exc} = 540 nm) for EB-DNA ([EB] = 20 μM, [DNA] = 26 μM) in buffer solution in the absence and presence of increasing amounts of complex **3** (up to the value of r = 0.42). The arrow shows the changes of intensity upon increasing amounts of **3**.

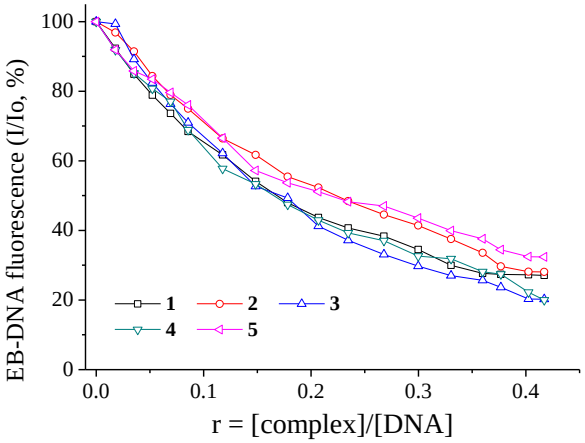

Figure S13. Plot of EB-DNA relative fluorescence intensity (I/Io, %) at λ_{em} = 592 nm *versus r* (*r* = [complex]/[DNA]) in buffer solution (150 mM NaCl and 15 mM trisodium citrate at pH 7.0) in the presence of complexes **1-5** (quenching up to 27.1% of the initial EB-DNA fluorescence for **1**, 28.1% for **2,** 22.3% for **3**, 20.0% for **4** and 32.4% for **5**).

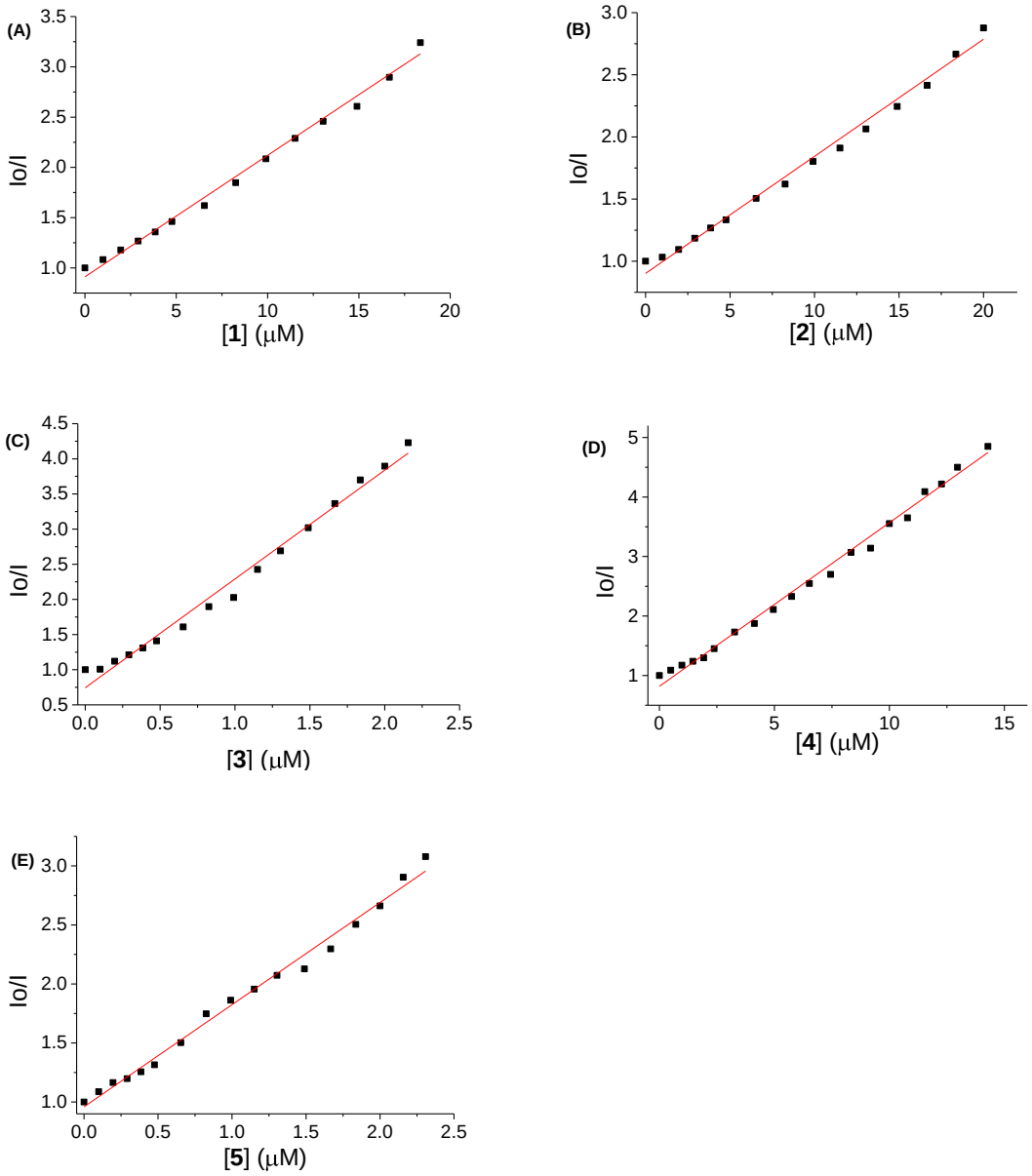

Figure S14. Stern-Volmer quenching plots of EB-DNA fluorescence for complexes (A)-(E) **1**-**5**, respectively.